Poisson–Boltzmann Theory for Membranes with Mobile Charged Lipids and the pH-Dependent Interaction of a DNA Molecule with a Membrane

Christian Fleck,* Roland R. Netz,† and Hans Hennig von Grünberg*
*Fakultät für Physik, Universität Konstanz, 78457 Konstanz, and †Max-Planck-Institut für Kolloid- und Grenzflächenforschung, 14424 Potsdam, Germany

ABSTRACT We consider a planar stiff model membrane consisting of mobile surface groups whose state of charge depends on the pH and the ionic composition of the adjacent electrolyte solution. To calculate the mean-field interaction potential between a charged object and such a model membrane, one needs to solve a Poisson–Boltzmann boundary value problem. We here derive and discuss the boundary condition at the membrane surface, a condition that is generally appropriate for biological membranes where two charge-regulating mechanisms are present at the same time: the pH-dependent chemical charge regulation and a regulation through the in-plane mobility of the surface groups. As an application of this general formalism, we consider the specific example of a single DNA molecule, approximated by a cylinder with smeared-out surface charges, interacting with such a model membrane. We study the effect that the two competing charge-regulating mechanisms have on the DNA/membrane interaction and the distribution of surface ions in the plane of the membrane. We find that, at short DNA–membrane distances, membrane fluidity can have a considerable impact on the DNA adsorption behavior and can lead to such counterintuitive phenomena as the adsorption of a negatively charged DNA onto a (on average) negatively charged membrane.

INTRODUCTION

Most biomembranes are charged. These charges arise from charged headgroups of phospholipids, adsorbed ions, and proteins. Phospholipids, the basic structural component of membranes, are charged due to the dissociation of protons. Depending on the charges of additional groups that may be bound to the phosphate group, phospholipids in water can have a valency between -2 and $+1$, and also neutral groups are possible (Cooper, 2000). The state of charge of a phospholipid is not a fixed quantity, but depends on the pH and the ionic composition of the adjacent electrolyte solution. For this reason, a specific phospholipid group is best characterized by a chemical-binding constant rather than by a fixed charge.

Biomembranes are usually in a fluid state in which individual membrane components are free to move in lateral directions, i.e., within the plane of the membrane, whereas their normal movements are highly restricted (Almeida and Vaz, 1995). Depending on their specific biological function, membranes are composed of mixtures of many different lipids and amphiphilic proteins, and it is, in particular, the proteins that are decisive for their specific function. However, if more general properties of membranes are concerned, it often makes sense to neglect this diversity (and especially the proteins), and to study a model membrane solely made of phospholipids (Sackman and Lipowsky, 1995).

Received for publication 8 May 2001 and in final form 10 September 2001.
Address reprint requests to Christian Fleck, Fakultät für Physik, Universität Konstanz, 78457 Konstanz, Germany. Tel.: +49-7531-883845; Fax: +49-7531-883157; E-mail: Christian.Fleck@uni-konstanz.de.

0006-3495/02/01/76/17 $2.00

In this article, we study such a model membrane. It is assumed to be a collection of surface groups, specified not other than that they can become charged and that they are mobile in the membrane plane. The membrane shape changes are neglected. Different types of groups are allowed for, each type being characterized by a chemical dissociation constant rather than a charge. With such a model, we take account of three basic properties of a lipid bilayer: that it may be composed of different types of phospholipids, that the state of charge of each surface group is controlled by a pH-dependent chemical reaction, and that the surface groups can diffuse laterally.

Specifically, this article addresses the question of how such a model membrane interacts electrostatically with other charged objects in an electrolyte solution. The interaction between charged macroscopic objects in an electrolyte solution is, in fact, an "effective" one (Löwen and Hansen, 2000), meaning that, in addition to the direct Coulomb interaction between both objects, there is a contribution to the interaction energy coming from the distance-dependent density distribution of the electrolyte ions around both objects. More precisely, the effective interaction can be viewed as the free energy of the whole system (composed of both macroions and microions) as a function of the distance between the macroions. In a mean-field approach, the essential input to calculate this free energy, and thus the effective interaction, is the electrostatic mean-field potential; it can be obtained from a Poisson–Boltzmann (PB) (Barrat and Joanny, 1996; Andelman, 1995) boundary value problem (BVP), where the boundaries are the surfaces of the two objects carrying the fixed charges. Important here is the choice of the boundary conditions, which must be made on physical grounds. Besides the constant-charge and constant-potential boundary condition, fixing either the potential or

its derivative at the boundary, a third boundary condition is well established, the charge-regulation boundary condition, where the surface charge is assumed not to be fixed, but to result from ionization of discrete surface sites (Ninham and Parsegian, 1971; Healy and White, 1978; Healy et al., 1980; Chan et al., 1976). The surface-charge density distribution is then a result, not a parameter, of the calculation; input parameters are rather the set of acid dissociation constants and the pH value.

This charge-regulation boundary condition is based on the assumption that the ionizable groups are locally fixed, and is thus not adequate for our case of a model membrane composed of mobile groups. This brings us to the major point of this paper. We derive a boundary condition for a PB BVP that goes beyond the traditional charge-regulation boundary condition by taking explicit account of surface group mobility. Once this point is clarified, the calculation of effective interactions is—though technically involved—conceptually simple. We then calculate the effective interactions between a charged rod and a charged membrane. Here we think of a DNA molecule interacting with a lipid membrane, which we see as a potential field of application of our results.

The issue of mobility of surface groups in an electrostatic context has been addressed before by Guttman and Andelman (1993) and Fogden and Ninham (1991), who investigated the interplay of a spontaneous curvature of a single membrane and the spatial modulation of the surface-charge density of mobile and immobile ions (Andelman, 1995). The effect of mobile surface charges has also been investigated treating the surface charges and counterions as strongly correlated two-dimensional (2D) liquids, which is a valid approximation at very large coupling parameters (i.e. low temperature or multivalent counterions) (Nguyen et al., 2000). Motivated by the recent interest in the DNA-cationic liposome complexes observed by Rädler et al. (1997) and Salditt et al. (1997), a sequence of theoretical papers appeared in which a periodic array of charged rods is considered that is adsorbed onto an oppositely charged surface with mobile charged groups (Menes et al., 1998; Dan, 1997; Bruinsma and Mashl, 1998; Harries et al., 2000; Wagner et al., 2000; Mashl et al., 1999; Mashl and Gronbech-Jensen, 1998). In the work of Harries et al. (2000), the appropriate boundary condition is derived by minimizing a free-energy functional. Quite recently, May et al. (2000a) considered the adsorption of charged proteins on membranes, taking explicit into account surface-group mobility. However, in all these works, the equilibrium between dissociated and associated surface groups was not considered. The case of a membrane consisting of equal amounts of negative and positive mobile lipids has been of special interest. The effective interaction between two fluid membranes is, in this case, solely due to correlation of in-plane charge fluctuations of mobile surface groups (Attard et al., 1988a; Pincus and Safran, 1998). The effect of such lateral charge fluctuations on the elastic properties of a membrane has been considered by Lau and Pincus (1998), and the effective interaction with test charges has been calculated using a generalized Green's formalism (Netz, 1999).

The outline of this paper is as follows. In the section Formulation of the Problem, we formulate the theoretical problem and present the results to make clear the underlying physics. The Theory section contains the formal solution that is derived from the grand-canonical partition function, a somewhat technical analysis that, however, is unnecessary to an understanding of the main result. In the Discussion, various simple limiting cases are considered to make the result more transparent and intuitively understandable. The next section is devoted to a typical application of our theory; we set up a PB BVP and calculate numerically the interaction of a charged cylinder approaching an oppositely charged wall consisting of mobile surface groups.

FORMULATION OF THE PROBLEM

We consider a charged surface S embedded in an aqueous electrolyte solution. In addition to the mobile electrolyte ions, there are ions on the surface that we assume to result from a dissociation of ionizable groups. We assume that there are M different types of such groups, each denoted by the symbol $A_i H_{\nu_i}$ ($i = 1, \ldots, M$). In water, these groups dissociate according to the reaction formula,

$$A_i H_{\nu_i} + \nu_i H_2O \rightleftharpoons A_i^{q_i} + \nu_i H_3O^+ \quad i = 1, \ldots, M, \quad (1)$$

where ν_i are the stoichiometric coefficients of the reaction and $A_i^{q_i}$ denote the negatively charged ions that remain at the surface. The valency of the ion of type i, q_i, is therefore $-\nu_i$. Each of the M different reactions in Eq. 1 is characterized by a dissociation constant K_s^i given by the law of mass action. For the moment, only simple acid reactions are allowed for, but generalization to basic groups is straightforward. Neutral surface groups are also included in the scheme, and can be realized by setting the corresponding dissociation constant equal to zero. We assume each surface group to cover some small area a^2 of the surface, which we assume to be the same area for every surface group type i. We can then regard the surface as being entirely composed of such groups. Every point on the surface belongs to one specific surface group. This leads to the idea of a regular lattice of site area a^2 being superposed on the surface, with each lattice site being occupied by one and only one surface group.

Inside the electrolyte solution and close to the surface, there is a charged object, which, for the moment, we need not specify further. Essential is that, in a mean-field description, the reduced electrostatic mean-field potential $\phi(\mathbf{r})$—that is, the potential multiplied by $e\beta$ with e being the elementary charge and $\beta = 1/kT$, the inverse temperature—is now a function of all three spatial dimensions.

Because of the presence of the charged object, there is a variation of $\phi(\mathbf{r})$ directly on the surface. Let us denote the position vector on the surface, $\mathbf{r} \in S$, by $\mathbf{r}_S$. Far away from the object, the surface potential $\phi(\mathbf{r}_S)$ approaches the constant value ϕ^∞. Note that this implies that the perturbation of the system due to the presence of the charged object is local.

What we calculate here is the partial surface density $\rho_i(\mathbf{r}_S)$ of the ion type $A_i^{q_i}$ for 1) a given surface potential $\phi(\mathbf{r}_S)$, 2) a given pH value of the electrolyte solution, and 3) a given set of dissociation constants K_s^i ($i = 1, \ldots, M$). This we want to do under the additional assumption that the surface groups are free to move in the surface. To set the stage, let us briefly consider the opposite case of immobile surface groups, where our task is easily solved. In case $\phi(\mathbf{r}_S) = \phi^\infty$, ρ_i is a constant, ρ_i^∞, and the law of mass action reads

$$K_s^i = \frac{\rho_i^\infty e^{\nu_i(-\mathrm{pH}\ln 10 - \phi^\infty)}}{c_i - \rho_i^\infty}, \tag{2}$$

with $\exp(-\mathrm{pH}\ln 10 - \phi^\infty)$ the concentration of H^+ ions at the surface, and c_i the number of surface ionizable groups of type i per area. Note that the concentration of water molecules is adsorbed into the definition of K_s^i. Hence,

$$\rho_i^\infty/c_i = (e^{\ln 10(\mathrm{pK}_s^i - \nu_i \mathrm{pH})} e^{q_i\phi^\infty} + 1)^{-1} \equiv \alpha_i, \tag{3}$$

where $\mathrm{pK}_s^i = -\ln K_s^i/\ln 10$. In the following, we refer to the ratio ρ_i^∞/c_i as the degree of dissociation α_i. For neutral surface groups ($K_s^i = 0$), the degree of dissociation becomes zero. If $\phi(\mathbf{r}_S)$ is now a function slowly varying on a length scale that is large compared to the lattice constant a of our regular lattice, then, Eqs. 2 and 3 should be valid for every single lattice cell and $\rho_i(\mathbf{r}_S)/c_i$ results from simply replacing $e^{q_i\phi^\infty}$ by $e^{q_i\phi(\mathbf{r}_S)}$ in Eq. 3. Expressing the resulting formula in terms of the degree of dissociation α_i defined in Eq. 3, one obtains

$$\frac{\rho_i(\mathbf{r}_S)}{c_i} = \frac{\alpha_i e^{-q_i\Delta\phi(\mathbf{r}_S)}}{(1-\alpha_i) + \alpha_i e^{-q_i\Delta\phi(\mathbf{r}_S)}}, \tag{4}$$

with $\Delta\phi(\mathbf{r}_S) = \phi(\mathbf{r}_S) - \phi^\infty$. In the same way, one obtains the surface density of the associated (A) groups $A_iH_{\nu_i}$ of type i, which we denote by $\rho_i^A(\mathbf{r}_S)$,

$$\frac{\rho_i^A(\mathbf{r}_S)}{c_i} = \frac{1-\alpha_i}{(1-\alpha_i) + \alpha_i e^{-q_i\Delta\phi(\mathbf{r}_S)}}. \tag{5}$$

Obviously,

$$\rho_i^A(\mathbf{r}_S) + \rho_i(\mathbf{r}_S) = c_i \tag{6}$$

for all points $\mathbf{r}_S$ on the surface. Eq. 4 then is the partial surface density $\rho_i(\mathbf{r}_S)$ for given values of pH and K_s^i and a given surface potential caused by the presence of the charged object in the vicinity of the membrane. The main message of the last three equations is that the degree to which a certain ionizable group dissociates, now depends on its position on the surface. As a result of such a spatial dependence of the degree of dissociation, a 2D surface-charge distribution forms. Eq. 6 states, in essence, that the surface groups are immobile; a group at $\mathbf{r}_S$ can dissociate or not, but it can never leave its position, so that the surface density of the dissociated and associated species must everywhere add up to c_i.

Things are different if the surface groups can freely move in the interfacial plane. There are now two possibilities for the surface groups to respond to the surface potential $\phi(\mathbf{r}_S)$. The first is the old one, the charge-regulation mechanism of adjusting the degree of dissociation to $\phi(\mathbf{r}_S)$, which is still effective, as in the case of immobile ions. However, in addition, the free energy of the system can now be lowered further by allowing the surface charges to move to their most favorable position in the 2D surface potential $\phi(\mathbf{r}_S)$.

The quantity that governs the movement of the surface groups is the set of chemical potentials μ_i for all types of surface groups. They regulate the exchange of surface groups with a reservoir. A change of sites between two groups of type i and j at lattice positions r_i and r_j is then to be understood as a process consisting of four steps: transferring particle at r_i to the reservoir (energy change $-\mu_i$), putting ion of type j from the reservoir to site r_i ($+\mu_j$), removing particle at r_j ($-\mu_j$) to the reservoir and inserting particle of type i at r_j (μ_i). The net energy change for a site change of two groups is thus zero, which is why we say that the groups can move freely. If, however, there is a $\mathbf{r}_S$ dependence of the surface potential, an exchange of sites can cause a change of energy, because it is now the $\mathbf{r}_S$-dependent electrochemical potential $\mu_i - q_i\phi(\mathbf{r}_S)$ rather than the chemical potential that regulates the exchange of sites.

With these few remarks, it should have become clear that the case of mobile surface groups is not simply a straightforward generalization of the results obtained for immobile ions, but that another charge-regulating mechanism is allowed for, and that more input parameters, as the chemical potentials of all groups, must now be incorporated into the theory. Starting from the grand-canonical partition function, we derive, in the next section, the following for the partial surface density of mobile ions of type i,

$$\rho_i(\mathbf{r}_S)a^2 = \frac{c_i a^2 \alpha_i e^{-q_i\Delta\phi(\mathbf{r}_S)}}{\sum_{j=1}^M c_j a^2((1-\alpha_j) + \alpha_j e^{-q_j\Delta\phi(\mathbf{r}_S)})}, \tag{7}$$

which is the pendant of Eq. 4, now for the case of mobile surface groups. We will also show that Eq. 5, for the case of mobile ions, becomes

$$\rho_i^A(\mathbf{r}_S)a^2 = \frac{c_i a^2 (1-\alpha_i)}{\sum_{j=1}^M c_j a^2((1-\alpha_j) + \alpha_j e^{-q_j\Delta\phi(\mathbf{r}_S)})}, \tag{8}$$

and one can recognize already that Eq. 6 is no longer valid, a feature that best shows the basic difference between the case of mobile and immobile ions. We continue this discussion after having derived Eqs. 7 and 8.

Once we know $\rho_i(\mathbf{r}_S)$ for all group types i, we can calculate the total surface charge density distribution $\rho_c(\mathbf{r}_S)$,

$$\rho_c(\mathbf{r}_S) = \sum_{i=1}^{M} q_i \rho_i(\mathbf{r}_S), \tag{9}$$

which, via Eq. 7, still depends on the 2D surface potential $\phi(\mathbf{r}_S)$. So far, we have assumed this surface potential to be a quantity known a priori. In practice, the spatially dependent electrostatic potential $\phi(\mathbf{r})$, and with it $\phi(\mathbf{r}_S)$, must be calculated in a self-consistent way from the PB BVP in which $\rho_c(\mathbf{r}_S)$ (and thus $\phi(\mathbf{r}_S)$) enter as boundary condition (see section DNA Near an Oppositely Charged Planar Membrane).

THEORY

We start with the grand partition function for a multicomponent electrolyte consisting of Q different types of ions, free to move in the three-dimensional configuration space $G\backslash G^*$, where G is the configuration space for the whole system and $G^* = S \cup C$. S is a 2D smooth manifold embedded in G, and C is the region occupied by an additional arbitrary distribution of fixed charges, denoted by $\sigma(\mathbf{r})$, located somewhere in $G\backslash S$. On S, we define an regular lattice, i.e., the area per site is constant. Each site is occupied by one out of M different surface groups. The area per site can be understood as the size of the surface group; all surface groups are thus assumed to be of the same size. A surface group on site i can be in one of two possible states (associated/dissociated), which yields in total $2M$ possible states per site. We label each site n with a state variable S_n similar to the spin variable in the Ising model. S_n can be any integer between 1 and $2M$. We introduce the particle density for the mobile electrolyte ions of type j in $G\backslash G^*$,

$$\rho_j^e(\mathbf{r}) = \sum_{k=1}^{N_j} \delta(\mathbf{r} - \mathbf{r}_k^j), \tag{10}$$

where $\mathbf{r}_k^j$ denotes the position vector of particle k of species j, and N_j the total number of particles of type j. Similarly, we write for the density of surface groups of type i in S,

$$\rho_i(\mathbf{r}) = \sum_{n=1}^{P} \delta_{iS_n} \delta(\mathbf{r} - \mathbf{r}_n). \tag{11}$$

Here, P is the number of lattice sites and $\mathbf{r}_n$ is the position vector of lattice site n. All together, we have three different sorts of ions, mobile electrolyte ions (density $\rho_j^e(\mathbf{r})$) in $G\backslash G^*$, fixed ions in $G\backslash S$ (density $\sigma(\mathbf{r})$) and charged/uncharged surface groups (density $\rho_i(\mathbf{r})$) in S, and the total charge density reads accordingly,

$$\rho^{tot}(\mathbf{r}) = \sum_{j=1}^{Q} q_j \rho_j^e(\mathbf{r}) + \sum_{i=1}^{2M} q_i \rho_i(\mathbf{r}) + \sigma(\mathbf{r}), \tag{12}$$

with q_i (q_j) being the valency of the surface groups (bulk ions) ($q_i = 0$ for an uncharged group). These charges interact via the Coulomb interaction, $\nu(\mathbf{r}, \mathbf{r}')$, so that the Hamiltonian of our system takes the simple form

$$H(\{\mathbf{r}_k^j\}, \{S_n\}) = \frac{1}{2} \int d\mathbf{r} \int d\mathbf{r}' \rho^{tot}(\mathbf{r}) \nu(\mathbf{r}, \mathbf{r}') \rho^{tot}(\mathbf{r}'). \tag{13}$$

We introduce the fugacities $\lambda_j = e^{\beta\mu_j}/\lambda_t^3$ and chemical potentials μ_j for the Q different types of bulk ions (λ_t the thermal wave length), and the fugacities and chemical potentials for the $2M$ different types of surface groups, $\lambda_i = e^{\beta\mu_i}/\lambda_t^2$ ($i = 1, \ldots, 2M$). The grand partition function of this system can then be written in the from,

$$\Xi = \prod_{j=1}^{Q} \sum_{N_j=0}^{\infty} \frac{\lambda_j^{N_j}}{N_j!} \int_{G\backslash G^*} \left[\prod_{k=1}^{N_j} d\mathbf{r}_k^j \right] \prod_{n=1}^{P} \sum_{S_n=1}^{2M} \left[\prod_{i=1}^{2M} \lambda_i^{\delta_{iS_n}} \right] \times e^{-H(\{\mathbf{r}_k^j\},\{S_n\})}. \tag{14}$$

With Eq. 14, we have brought our problem into a form well suited for applying standard field-theoretical methods. The details of what follows now are not specific to this calculation, and has been described elsewhere; we refer the reader, for example, to Netz and Orland (1999, 2000) Netz (1999, 2000), and continue with a more condensed description of the calculation. After renormalizing the fugacities to get rid of diagonal terms, a Hubbard–Stratonovich transformation leads us to

$$\Xi = \prod_{j=1}^{Q} \sum_{N_j=0}^{\infty} \frac{\lambda_j^{N_j}}{N_j!} \int \frac{\mathcal{D}\psi}{\sqrt{\det \nu}} \int_{G\backslash G^*} \left[\prod_{k=1}^{N_j} d\mathbf{r}_k^j \right] \times \prod_{n=1}^{P} \sum_{S_n=1}^{2M} \left[\prod_{i=1}^{2M} \lambda_i^{\delta_{iS_n}} \right] e^{-H(\psi,\{\mathbf{r}_k^j\},\{S_n\})}, \tag{15}$$

where

$$H(\psi, \{\mathbf{r}_k^j\}, \{S_n\}) = \frac{k_B T}{8\pi e^2} \int_G d\mathbf{r} (\nabla\psi(\mathbf{r}))^2 \varepsilon(\mathbf{r}) + \int_G d\mathbf{r} \rho^{tot}(\mathbf{r}) i\psi(\mathbf{r}) - \int_{G\backslash G^*} d\mathbf{r} \sum_{j=1}^{Q} \rho_j^e(\mathbf{r}) h_j(\mathbf{r}) - \int_S \sum_{i=1}^{2M} \rho_i(\mathbf{r}) h_i(\mathbf{r}), \tag{16}$$

with ψ being a fluctuating field and $\varepsilon(\mathbf{r})$ a dielectric field defined on G. To be able to calculate later the expectation

values of the charge density operators, we introduce at this point, the generating fields $h_i(\mathbf{r})$ and $h_j(\mathbf{r})$, which couple to the densities $\rho_i(\mathbf{r})$ and $\rho_j^e(\mathbf{r})$, respectively. Resolving our abbreviations in Eq. 16, Eqs. 10, 11, and 12, performing the sums and making use of the series expansion of the exponential function, we can bring the partition function into the form,

$$\Xi = \int \frac{\mathcal{D}\psi}{\sqrt{\det \nu}} e^{-H_G[\psi]} \prod_{n=1}^{P} \sum_{S_n=1}^{2M} \prod_{i=1}^{2M} (\lambda_i e^{h_i(\mathbf{r}_n) - iq_i\psi(\mathbf{r}_n)})^{\delta_{iS_n}},$$

with the abbreviation

$$H_G[\psi] := \frac{k_B T}{8\pi e^2} \int_G d\mathbf{r} (\nabla\psi(\mathbf{r}))^2 \varepsilon(\mathbf{r}) + \int_G d\mathbf{r}\sigma(\mathbf{r}) i\psi(\mathbf{r}) - \sum_{j=1}^{Q} \lambda_j \int_{G\backslash G^*} d\mathbf{r} e^{h_j(\mathbf{r}) - q_j i\psi(\mathbf{r})}. \quad (17)$$

This can be further simplified to

$$\Xi = \int \frac{\mathcal{D}\psi}{\sqrt{\det \nu}} e^{-H_G[\psi]} \prod_{n=1}^{P} \sum_{i=1}^{2M} (\lambda_i e^{h_i(\mathbf{r}_n) - iq_i\psi(\mathbf{r}_n)}). \quad (18)$$

If the physical properties of the system vary on a much larger scale than the size of a lattice site, we can avoid the sum over a discrete lattice. Introducing the functional,

$$H_S[\psi] := \frac{-1}{a^2} \int_S d\mathbf{r} \ln\left(\sum_{i=1}^{2M} \lambda_i e^{h_i(\mathbf{r}) - iq_i\psi(\mathbf{r})} \right), \quad (19)$$

we can rewrite Eq. 18 as

$$\Xi = \int \frac{\mathcal{D}\psi}{\sqrt{\det \nu}} e^{-H_G[\psi] - H_S[\psi]}. \quad (20)$$

We approximate the integral over all possible configurations by the configuration for which the partition function is stationary (saddle-point approximation),

$$\Xi_{SP} = e^{-H_G[\psi_{SP}] - H_S[\psi_{SP}]}, \quad (21)$$

where the mean-field potential ψ_{SP} results from,

$$\left. \frac{\delta(H_G + H_S)}{\delta\psi(\mathbf{r})} \right|_{\substack{\psi=\psi_{sp} \\ h_i=h_j=0}} = 0. \quad (22)$$

From the mean-field partition function, Eq. 21, we can now derive all quantities needed for the following. We start with the densities of the electrolyte ions; it can be obtained with the help of the functions $h_j(\mathbf{r})$,

$$\rho_j^e(\mathbf{r}) = \left. \frac{\delta \ln \Xi_{SP}}{\delta h_j(\mathbf{r})} \right|_{h_i=h_j=0} \quad \mathbf{r} \in G\backslash G^*, \quad (23)$$

which yields

$$\rho_j^e(\mathbf{r}) = \lambda_j e^{-q_j\phi(\mathbf{r})} \quad \mathbf{r} \in G\backslash G^*, \quad (24)$$

where we have introduced $\phi := i\psi_{SP}$. The bulk ion fugacities λ_j may be determined from the ion densities far way from the surface S and the fixed charge distribution σ where one may safely assume that $\rho_j^e(\mathbf{r}_\infty) = c_j^e$ with c_j^e being the concentration of electrolyte ions of type j ($\sum_{j=1}^{Q} q_j c_j^e = 0$). This leads to $\lambda_j = c_j^e$. The densities of the surface groups in mean-field approximation can be calculated from ($\mathbf{r}_S = \mathbf{r} \in S$)

$$\rho_i(\mathbf{r}_S) = \left. \frac{\delta \ln \Xi_{SP}}{\delta h_i(\mathbf{r}_S)} \right|_{h_i=h_j=0}, \quad (25)$$

resulting in the expression

$$\rho_i(\mathbf{r}_S) = \frac{1}{a^2} \frac{\lambda_i e^{-q_i\phi(\mathbf{r}_S)}}{\sum_{j=1}^{2M} \lambda_j e^{-q_j\phi(\mathbf{r}_S)}}. \quad (26)$$

Again the fugacities need to be determined. Henceforth, we denote the density of the associated species by ρ_i^A, the fugacity of the associated species by λ_i, and that of the dissociated one by $\lambda_i\lambda_i^D$ ($i \in \{1, \ldots, M\}$, $\lambda_i^D = e^{\beta\mu^D}$). Furthermore, we set the valencies of the neutral surface groups to zero. For $\mathbf{r}_S$ far away from any fixed charge distribution $\sigma(\mathbf{r})$ we expect a homogeneous density,

$$a^2\rho_i^\infty + a^2\rho_i^{\infty A} = a^2 c_i = \frac{\lambda_i(\lambda_i^D e^{-q_i\phi^\infty} + 1)}{\sum_{j=1}^{M} \lambda_j(\lambda_j^D e^{-q_j\phi^\infty} + 1)}, \quad (27)$$

and hence,

$$\lambda_i = \frac{a^2 c_i}{1 - a^2 c_i} \frac{\sum_{j\neq i}^{M} \lambda_j(\lambda_j^D e^{-q_j\phi^\infty} + 1)}{\lambda_i^D e^{-q_i\phi^\infty} + 1}. \quad (28)$$

This is an eigenvalue equation for the fugacities for the eigenvalue 1 with the eigenvector,

$$\lambda_i = \frac{c_i a^2}{1 + \lambda_i^D e^{-q_i\phi^\infty}}. \quad (29)$$

We determine the λ_i^D by means of the mass action law, Eqs. 2 and 3. At infinity, the ratio of ρ_i^∞ and $\rho_i^{\infty A} = c_i - \rho_i^\infty$ must

be equal to $\alpha_i/(1-\alpha_i)$ as defined in Eq. 3. In contrast, Eq. 26 yields $\rho_i^{\infty}/\rho_i^{\infty A} = \lambda_i^D e^{-q_i\phi^{\infty}}$ so that

$$\lambda_i^D = e^{q_i\phi^{\infty}} \frac{\alpha_i}{1-\alpha_i}. \tag{30}$$

Inserting the expression for λ_i and λ_i^D in Eq. 26 leads us directly to the main result of this paper, Eqs. 7 and 8.

The mean-field partition function provides us also with the grand potential Ω,

$$\beta\Omega = -\ln \Xi_{SP}\Big|_{h_i=h_j=0} = H_G[\phi/i] + H_S[\phi/i]\Big|_{h_i=h_j=0}. \tag{31}$$

It is important to realize that this equation is only valid if we use the mean-field potential defined by Eq. 22 in H_G and H_S. Using Eqs. 17 and 19, we obtain for the grand potential

$$\begin{aligned}\beta\Omega = &-\frac{k_BT}{8\pi e^2}\int_G d\mathbf{r}(\nabla\phi(\mathbf{r}))^2\varepsilon(\mathbf{r}) \\ &+ \int_G d\mathbf{r}\sigma(\mathbf{r})\phi(\mathbf{r}) - \sum_{j=1}^{Q} c_j^e \int_{G\backslash G^*} d\mathbf{r} e^{-q_j\phi(\mathbf{r})} \\ &- \frac{1}{a^2}\int_S d\mathbf{r}\ln\left(\sum_{i=1}^{M} a^2 c_i(\alpha_i e^{-q_i\Delta\phi(\mathbf{r})} + (1-\alpha_i))\right).\end{aligned} \tag{32}$$

An interesting property of the system is that the partition function factorizes due to the mean-field description,

$$\Xi_{SP} = Z_G[\phi]Z_S[\phi], \tag{33}$$

with $Z_G[\phi] := \exp\{-H_G[\phi/i]\}$ and $Z_S[\phi] := \exp\{-H_S[\phi/i]\}$. Therefore, it is easy to extend our model to several independent lattice systems. Let us denote the kth of these lattices by S_k. The partition function for each lattice factorizes itself and is just the product of the partition functions of each single lattice site as can be seen in Eq. 18. Allowing on S_k, $2M_k$ different states on each site, we get for the partition sum of this sub-system Z_{S_k}

$$Z_{S_k} = \prod_{n=1}^{P_k}\sum_{i=1}^{2M_k} \lambda_i^k e^{h_i^k(\mathbf{r}_n^k) - q_i^k\phi(\mathbf{r}_n^k)}, \tag{34}$$

which, for a slowly varying field ϕ, can be approximated by

$$Z_{S_k} = \exp\left\{\frac{1}{a_k^2}\int_{S_k} d\mathbf{r}\ln\left(\sum_{i=1}^{2M_k}\lambda_i^k e^{h_i^k(\mathbf{r}) - q_i^k\phi(\mathbf{r})}\right)\right\}. \tag{35}$$

It is not needed that the lattices are spatially distinct. Due to this property, we are capable of describing a system of several interpenetrating lattices and thus modeling a surface with various immobile surface groups. The partition function for a system with L different lattices hence reads,

$$\Xi_{SP} = Z_G[\phi]\prod_{k=1}^{L} Z_{S_k}[\phi]. \tag{36}$$

If we determine the fugacities for each lattice similar to the procedure for one lattice done above, we arrive at the following expression for the grand potential:

$$\begin{aligned}\beta\Omega = &-\frac{k_BT}{8\pi e^2}\int_G d\mathbf{r}(\nabla\phi(\mathbf{r}))^2\varepsilon(\mathbf{r}) + \int_G d\mathbf{r}\sigma(\mathbf{r})\phi(\mathbf{r}) \\ &- \sum_{j=1}^{Q} c_j^e \int_{G\backslash G^*} d\mathbf{r} e^{-q_j\phi(\mathbf{r})} - \sum_{k=1}^{L}\frac{1}{a_k^2}\int_{S_k} \\ &\times d\mathbf{r}\ln\left(\sum_{i=1}^{M_k} a_k^2 c_i^k(\alpha_i^k e^{-q_i^k\Delta\phi(\mathbf{r})} + (1-\alpha_i^k))\right),\end{aligned} \tag{37}$$

where G^* now becomes $\cup_{k=1}^{L} S_k \cup C$. If we specialize to one ionizable surface group on each lattice, i.e., two different states on each lattice site ($M_k = 1$), we readily arrive at the densities given by Eqs. 4 and 5 above.

Note that it is an inherent assumption for our present treatment of the model, that the fixed charge distribution perturbs the surfaces S_k only locally. Only under this condition we can chose the fugacities in the way we did above. Furthermore, we can show that, in the case of local perturbation, the relative number fluctuation of the particle of type i in the surface goes like $1/\sqrt{N}$, where N is the total number of particle in the surface. Thus, in the case of large particle numbers, i.e. large surfaces, our description of the system is equivalent to the case where the particle numbers are fixed.

DISCUSSION

Having derived the two expressions, Eqs. 7 and 8, we now want to convey a more intuitive understanding of their meaning. For that purpose, we consider a few simple cases. We re-iterate beforehand that our result relies on the existence of a regular lattice with lattice constant a superposed on the surface, and that it is thus valid only if one can assume that all membrane components are of the same size and arrangeable on such a lattice. In both Eqs. 7 and 8, a^2 appears in conjunction with surface densities c_i (or ρ_i), and the product c_ia^2 (ρ_ia^2) can be understood just as the surface fraction of species i. Because the surface is closely packed with groups, $\sum_{j=1}^{M} c_ja^2 = 1$.

The simplest case is that the potential does not depend on the surface position vector $\mathbf{r}_S$, either because the charged surface is well separated from other charged objects in the solution, or because of symmetry reasons (e.g., two parallel planar walls). Then $\Delta\phi(\mathbf{r}_S) = 0$ and Eqs. 7 and 8 reduce to

$\rho_i(\mathbf{r}_S)/c_i = \alpha_i$ and $\rho_i^A(\mathbf{r}_S)/c_i = 1 - \alpha_i$. The same result is obtained if the surface groups are immobile (insert $\Delta\phi(\mathbf{r}_S) = 0$ in Eqs. 4 and 5). If there is no variation of the potential on the surface, there is no point in distinguishing between mobile and immobile surface groups; the mean-field potential is the same for both cases. This implies, for example, that the effect of mobility of surface groups cannot be studied in problems depending only on the spatial coordinate z on the mean-field level, as, for example, the traditional Gouy–Chapman problem of a single-charged wall bordering to an electrolyte solution.

If $\Delta\phi(\mathbf{r}_S)$ is now taken to be a spatially varying function, then there is a difference between mobile and immobile surface groups, best to be seen from the following consideration. The total surface density of groups of type i at $\mathbf{r}_S$, $\rho_i(\mathbf{r}_S) + \rho_i^A(\mathbf{r}_S)$, is usually not equal to c_i, as can be seen by adding Eq. 7 to Eq. 8. Because c_i is the total surface density of groups when $\Delta\phi(\mathbf{r}_S) = 0$ (i.e., before switching on $\phi(\mathbf{r}_S)$), groups of type i must have moved after $\phi(\mathbf{r}_S)$ was switched on, either by disappearing from or by coming to the point $\mathbf{r}_S$. This is in direct contrast to the case of immobile ions where the total surface density of groups of type i remains unaffected by $\phi(\mathbf{r}_S)$, and is always equal to c_i, see Eq. 6. Mobility of surface groups, however, does not mean that sites on the surface remain unoccupied:

$$\sum_{j=1}^{M} (\rho_j(\mathbf{r}_S)a^2 + \rho_j^A(\mathbf{r}_S)a^2) = \sum_{j=1}^{M} c_j a^2 = 1, \qquad (38)$$

which shows that the lattice site at $\mathbf{r}_S$ is always occupied by some surface groups, though not necessarily by that specific group it was occupied before $\Delta\phi(\mathbf{r}_S)$ became nonzero.

We next remark that the distinction between mobile and immobile ions is again pointless if only one type of surface group is present, because the exchange of sites of two identical groups can have no energetic effect, and, indeed, Eqs. 7, 8, and 38 reduce to Eqs. 4, 5, and 6 if $M = 1$.

Let us now consider a surface composed of two types of mobile surface groups, the first of which can dissociate (degree of dissociation $\alpha_1 = \alpha$), the second not ($\alpha_2 = 0$). With Eqs. 7 and 9, we then find for the total surface charge density,

$$\rho_c(\mathbf{r}_S)a^2 = q_1\rho_1(\mathbf{r}_S)a^2 = \frac{q_1 c_1 a^2 \alpha e^{-q_1\Delta\phi(\mathbf{r}_S)}}{c_1 a^2 \alpha e^{-q_1\Delta\phi(\mathbf{r}_S)} + (1 - c_1 a^2 \alpha)}, \qquad (39)$$

where we have used $(c_1 + c_2)a^2 = 1$. Specializing this expression further to the case $\alpha = 1$,

$$\rho_c(\mathbf{r}_S)a^2 = \frac{q_1 c_1 a^2 e^{-q_1\Delta\phi(\mathbf{r}_S)}}{c_1 a^2 e^{-q_1\Delta\phi(\mathbf{r}_S)} + (1 - c_1 a^2)}, \qquad (40)$$

we have the surface charge density resulting only from the mobility of the groups. If, in contrast, we allow for only one type of surface group by setting $c_1 a^2 = 1$, then Eq. 39 reduces to

$$\rho_c(\mathbf{r}_S)a^2 = \frac{q_1 \alpha e^{-q_1\Delta\phi(\mathbf{r}_S)}}{\alpha e^{-q_1\Delta\phi(\mathbf{r}_S)} + (1 - \alpha)}, \qquad (41)$$

which is identical to the expression one obtains starting from Eq. 4 for immobile groups. Eq. 41 thus represents the case of a surface charge density generated by a $\mathbf{r}_S$-dependent dissociation of one type of ions, no matter if mobile or not. Both Eqs. 40 and 41 appeared in literature before: Eq. 40 has been derived by Harries et al. (2000) (see also (May et al., 2000a)), whereas Eq. 41 is the starting point of the classical paper of Ninham and Parsegian (1971) introducing the concept of the charge-regulation PB boundary condition.

Comparison of Eqs. 40 and 41 reveals the close relationship between dissociation and surface group mobility as the two basic charge-regulating mechanisms: Eq. 40 becomes identical to Eq. 41 if one sets the surface fraction $c_1 a^2$ in Eq. 40 equal to the degree of dissociation α in Eq. 41. This is not surprising, because α measures the fraction of ions relative to the total number of groups, exactly as $c_1 a^2$ does in the mixture of neutral and charged groups. Thus, we see that the case of a mixture of neutral and fully dissociated mobile surface groups is equivalent to the case of a surface made of one type of dissociable groups, and can be brought into correspondence by interpreting the surface fraction in the first case as a degree of dissociation for the second case. Even the more general case of Eq. 39 can be understood as yet another realization of the old Ninham/Parsegian case, if one interprets $c_1 a^2 \alpha$ in Eq. 39 as an "effective" dissociation constant. However, these are the only cases where this equivalence can be found. Both effects, mobility and dissociation, are present at the same time and can usually not be unified by introducing an effective degree of dissociation.

Let us now turn to another interesting example, a 2D salt solution, a notion that only recently has been introduced in the context of biomembranes (Pincus and Safran, 1998). We consider a surface composed of two sorts of fully dissociated surface groups ($\alpha_1 = \alpha_2 = 1$) of opposite charge, $q_1 = -q_2 = q$. Eq. 7 then leads to

$$\rho_c(\mathbf{r}_S)a^2 = qa^2(\rho_1(\mathbf{r}_S) - \rho_2(\mathbf{r}_S)) = q\,\frac{c_1 a^2 e^{-q\Delta\phi(\mathbf{r}_S)} - (1 - c_1 a^2)e^{q\Delta\phi(\mathbf{r}_S)}}{c_1 a^2 e^{-q\Delta\phi(\mathbf{r}_S)} + (1 - c_1 a^2)e^{q\Delta\phi(\mathbf{r}_S)}}, \qquad (42)$$

which becomes

$$\rho_c(\mathbf{r}_S)a^2 = -q \tanh q\Delta\phi(\mathbf{r}_S), \qquad (43)$$

if $c_1 a^2 = c_2 a^2 = \frac{1}{2}$. If $\Delta\phi(\mathbf{r}_S) = 0$, the surface-charge density in Eq. 43 becomes zero. If, however, there is a perturbation of the surface potential due to the presence of another charged object, then the surface ions are taking part in a 2D screening of the object and escape from, or assemble in,

regions where $\Delta\phi(\mathbf{r}_S)$ departs from zero. The surface is then locally charged.

To give an alternative access to our results, let us reformulate Eqs. 7 and 8 in terms of chemical potentials. With $\alpha_i = \rho_i^\infty/c_i$, Eq. 30 becomes

$$e^{\beta\mu_i^D} = \lambda_i^D = \frac{\rho_i^\infty e^{q_i\phi^\infty}}{c_i - \rho_i^\infty}, \tag{44}$$

which we insert in Eq. 29 to find the chemical potentials of the associated surface groups,

$$\frac{e^{\beta\mu_i}}{e^{\beta\mu_M}} = \frac{c_i - \rho_i^\infty}{c_M - \rho_M^\infty}. \tag{45}$$

The charged groups are sensitive to the surface potential, and we thus have to consider the electrochemical potential,

$$\beta\mu_{el,i}(\mathbf{r}_S) = \beta\mu_i + \beta\mu_i^D - q_i\phi(\mathbf{r}_S), \tag{46}$$

which is $\mathbf{r}_S$-dependent if $\Delta\phi(\mathbf{r}_S) \neq 0$. Inserting Eqs. 45 and 46 in Eq. 44, one obtains

$$\frac{e^{\beta\mu_{el,i}^\infty}}{e^{\beta\mu_{el,M}^\infty}} = \frac{\rho_i^\infty}{\rho_M^\infty}. \tag{47}$$

These equations provide us with an expression for c_i/c_j in terms of the chemical/electrochemical potentials, and Eqs. 7 and 8 can then be brought into the form,

$$\rho_i(\mathbf{r}_S)a^2 = \frac{e^{\beta\mu_{el,i}(\mathbf{r}_S)}}{\sum_{j=1}^M (e^{\beta\mu_j} + e^{\beta\mu_{el,j}(\mathbf{r}_S)})}, \tag{48}$$

and

$$\rho_i^A(\mathbf{r}_S)a^2 = \frac{e^{\beta\mu_i}}{\sum_{j=1}^M (e^{\beta\mu_j} + e^{\beta\mu_{el,j}(\mathbf{r}_S)})}. \tag{49}$$

These two expressions lead us to a simple statistical explanation of our result, suggested by the fact that the denominators in both expressions have the appearance of partition functions. Changing from the continuous description to a discrete counting of surface groups, $\mathbf{r}_S \to \mathbf{r}_n$, one may regard every single surface group at $\mathbf{r}_n$ as an independent subsystem. Each surface site $\mathbf{r}_n$ is occupied by a group which can be in one of $2M$ possible energy states, $\mu_{el,1}(\mathbf{r}_n) \ldots \mu_{el,M}(\mathbf{r}_n)$, $\mu_1, \ldots, \mu_M$. The partition function of this subsystem then is

$$Z_n = \sum_{j=1}^M (e^{\beta\mu_j} + e^{\beta\mu_{el,j}(\mathbf{r}_n)}), \tag{50}$$

from which the probability P of finding the particle in state $\mu_{el,i}(\mathbf{r}_n)$ follows according to the basic rules of statistical mechanics,

$$P(\mu_{el,i}(\mathbf{r}_n)) = e^{\beta\mu_{el,i}(\mathbf{r}_n)}/Z_n. \tag{51}$$

This is Eq. 48, which is thus understood as the probability that the surface group is in one specific discrete energy state out of $2M$ possible, namely in the state $\mu_{el,i}(\mathbf{r}_n)$. Accordingly, Eq. 49 is interpreted as the probability of finding the surface group in one of the energy states μ_i corresponding to an associated group. Regarding the surface as a collection of independent subsystems, one at each lattice site, the partition sum of the whole system can be obtained as a product of Eq. 50 over all lattice sites. This leads us back to Eq. 34. Allowing in the sums of Eqs. 48 and 49 only the term $j = i$ gives us the equivalent expressions for the case of immobile ions. The basic difference between immobile and mobile ions, then, is that, for immobile ions, we have M noninteracting sublattices with two possible states on each site, whereas, for mobile groups, we have just one lattice with $2M$ states on each site.

This interpretation is very intriguing because it allows a direct generalization of our result to the three-dimensional (3D) case. Consider an aqueous q_+:q_- electrolyte solution in bulk. Suppose the volume of the solution is divided into small cells, with each cell of volume a^3 being occupied by either a water molecule or a negative ion or a positive ion. The concentration (volume fraction) of either ion type is c_b ($c_b a^3$). In each cell, there is thus either a water molecule having the chemical potential $\beta\mu_w$ or a positive (negative) ion having the electrochemical potential $\beta\mu_{ion} - q_\pm\phi(\mathbf{r})$. As in Eqs. 45 and 47, the chemical potentials are given by the ratio between the volume fraction of water ($1 - 2c_b a^3$) and the volume fraction of one ion type, $\exp(\beta(\mu_{ion} - \mu_w)) = c_b a^3/(1 - 2c_b a^3)$. The probability $P(\pm)$ of finding the cell at position $\mathbf{r}$ being occupied by a particle in state $\mu_{ion} - q_\pm\phi(\mathbf{r})$, i.e., by a positive or negative ion, is

$$\begin{aligned} P(\pm) &= \frac{e^{(\beta\mu_{ion} - q_\pm\phi(\mathbf{r}))}}{e^{(\beta\mu_{ion} - q_+\phi(\mathbf{r}))} + e^{(\beta\mu_{ion} - q_-\phi(\mathbf{r}))} + e^{\beta\mu_w}} \\ &= \frac{c_b a^3 e^{-q_\pm\phi(\mathbf{r})}}{c_b a^3(e^{-q_+\phi(\mathbf{r})}) + e^{-q_-\phi(\mathbf{r})} + 1 - 2c_b a^3}, \end{aligned} \tag{52}$$

which is obviously the generalization to 3D of Eq. 51. For $q_+ = -q_- = 1$, this leads to a density

$$\begin{aligned} \rho(\mathbf{r})a^3 &= P(+) - P(-) \\ &= \frac{-2c_b a^3 \sinh\phi(\mathbf{r})}{2c_b a^3 \cosh\phi(\mathbf{r}) + 1 - 2c_b a^3}, \end{aligned} \tag{53}$$

which, when placed into the Poisson equation $\nabla^2\phi = -4\pi\lambda_B\rho$, yields the modified PB equation suggested by Borukhov et al. (Borukhov et al., 1997, 2000; Kralj-Iglic and Iglic, 1996). It takes account of steric effects in electrolytes, and is thus an attempt to overcome one of the major deficiency of standard PB theory, the point-charge approximation, which leads to an unphysically high charge density near charged surfaces, (see Borukhov et al., 1997). Having thus shown the close relationship between our 2D result and the 3D calculation of Borukhov et al. (1997) we now want to set up and solve a full PB BVP.

DNA NEAR AN OPPOSITELY CHARGED PLANAR MEMBRANE

The density distribution of the dissociated and associated surface groups, Eqs. 7 and 8, depends on the potential at the surface that has a spatial dependence due to the presence of a charged object near the surface. We now formulate a PB BVP where Eqs. 7 and 8 appear as boundary conditions, and calculate the effective interaction between the object and the surface. As an example, we choose the model system of an infinitely long charged rod interacting with an oppositely charged plane that is densely packed with mobile surface groups. Such a system is realized, for example, by an anionic DNA strand interacting with a supported cationic lipid bilayer, something that has been studied extensively in recent years (Fang and Yang, 1997; Lasic et al., 1997; Maier and Rädler, 1999; Gelbart et al., 2000). Stable multilamellar aggregates of DNA with cationic liposomes have been identified (Lasic et al., 1997; Rädler et al., 1997; Koltover et al., 1998, 1999; Salditt et al., 1997), which are of special interest because they are possible candidates for nonviral gene-therapy strategies and can serve as vehicles to transport DNA into cells (Firshein, 1989; Behr, 1994; Verma and Somia, 1997; Felgner et al., 1987, 1994; Templeton et al., 1997). Theoretical studies on the stability and organization of such complexes have appeared in literature (Dan, 1997; Harries et al., 2000; Bruinsma and Mashl, 1998), focusing in particular on such issues as the counterion release force (Fleck and von Grünberg, 2001; Sens and Joanny, 2000; Bruinsma and Mashl, 1998; Wagner et al., 2000), the evolution of phases of these complexes (May et al., 2000b; Harries et al., 2000), salt effects on effective interactions (Parsegian and Gingell, 1972; Mashl et al., 1999), and the effect of surface ion mobility on screening (Menes et al., 1998). Numerous other theoretical and experimental adsorption studies of polyelectrolytes other than DNA can be found in Fleer et al. (1993).

In particular, it has been shown that spatial inhomogeneities in the membrane surface-charge density in response to interactions with the DNA can have a significant effect on the phase behavior and stability of DNA/cationic lipid complexes (Harries et al., 2000). However, only whole complexes of DNA plus membranes have been studied theoretically, but never the problem of a single DNA molecule in interaction with a membrane. Against this background, the example considered in this section is certainly useful not only to clarify the usage of Eqs. 7 and 8 in an effective-interaction calculation, but also to study exemplarily the effect of surface-group mobility for a single DNA interacting with a lipid membrane. Important in the following is the pH-dependent charge fraction parameter $\alpha_i = \rho_i^\infty/c_i$, which, for simplicity, we take as an independent input parameter in the following calculations. If one wishes to apply our results to a specific membrane, one first has to formulate the specific charge-regulating chemical reaction at the membrane's surface (which need not be our Eq. 1), then write down the law of mass action as in Eq. 2, and use this to define α_i in the same way as we have done in Eq. 3 for our reaction in Eq. 1. The inset of Fig. 6 shows the degree of dissociation α_1 as a function of the difference $pK_s - pH$ for a specific choice of parameters.

We now assume that the surface S in the Theory section is the x–y plane at $z = 0$, which divides the configuration space into two parts, an aqueous 1:1 electrolyte solution of salt concentration c_s in $G_> = \{\mathbf{r}|z > 0\}\backslash G_z$ (G_z region of the cylinder) with a dielectric constant $\varepsilon_>$, and a dielectric medium with a dielectric constant $\varepsilon_<$ at $z < 0$ ($G_<$). A cylinder, having a radius r_0, a line charge density τ, and being made of a material with a dielectric constant ε_z, is located at ($x = 0$, $z = h$), with its axis parallel to the y-axis. The dielectric field is thus given by,

$$\varepsilon(\mathbf{r}) = \varepsilon_>\theta(z)\theta(c(\mathbf{r})) + \varepsilon_<\theta(-z) + \varepsilon_z\theta(-c(\mathbf{r})), \quad (54)$$

with $\theta(-c(\mathbf{r}))$ and $c(\mathbf{r}) = \sqrt{x^2 + (z-h)^2} - r_0$ determining the region G_z of the cylinder. Eq. 22 then gives, with Eqs. 29 and 30,

$$\begin{aligned} 0 = &-\frac{k_B T}{4\pi e^2}\nabla(\varepsilon(\mathbf{r})\nabla\psi(\mathbf{r})) + i\sigma(\mathbf{r}) \\ &+ ic_s\theta(z)\theta(c(\mathbf{r}))e^{-i\psi(\mathbf{r})} \\ &- ic_s\theta(z)\theta(c(\mathbf{r}))e^{+i\psi(\mathbf{r})} \\ &+ i\frac{\delta(z)}{a^2}\frac{\sum_{i=1}^{M} q_i c_i a^2 \alpha_i e^{-iq_i\Delta\psi(r)}}{\sum_{i=1}^{M} c_i a^2(\alpha_i e^{-iq_i\Delta\psi(r)} + (1-\alpha_i))}, \end{aligned} \quad (55)$$

where $\Delta\psi := \psi - \phi^\infty/i$. The charge distribution of fixed charges is now given by the charges on the cylinder surface, $\sigma(\mathbf{r}) = -\tau\delta(c(\mathbf{r}))/2\pi r_0$. We furthermore assume $\varepsilon_</\varepsilon_> \to 0$ and $\varepsilon_z/\varepsilon_> \to 0$, because water has an extraordinarily high dielectric constant compared to most other materials. Writing $\phi = i\psi_{SP}$, with ψ_{SP} satisfying Eq. 55, and using the definition of $\varepsilon(\mathbf{r})$ (Eq. 54), we arrive at the following PB BVP:

$$\begin{aligned} \Delta\phi(\mathbf{r}) &= \kappa^2 \sinh\phi(\mathbf{r}) && \mathbf{r} \in G_> \\ \mathbf{n}_z\nabla\phi(\mathbf{r}) &= 2\lambda_B\tau/r_0 && \mathbf{r} \in \partial G_z \\ \mathbf{n}_=\nabla\phi(\mathbf{r}) &= -4\pi\lambda_B\rho_c(\mathbf{r}) && \mathbf{r} \in S, \end{aligned} \quad (56)$$

with

$$\rho_c(\mathbf{r}) = \frac{\sum_{i=1}^{M} q_i c_i \alpha_i e^{-q_i\Delta\phi(\mathbf{r})}}{\sum_{i=1}^{M} c_i a^2(\alpha_i e^{-q_i\Delta\phi(\mathbf{r})} + (1-\alpha_i))}, \quad (57)$$

and $\lambda_B := e^2\beta/\varepsilon_>$, ∂G_z for the cylinder surface and $\kappa^2 = 8\pi\lambda_B c_s$. $\mathbf{n}_z$ and $\mathbf{n}_=$ are two unit vectors, normal to the surfaces ∂G_z and S, respectively, and pointing both into the region $G_>$. Note that Eq. 57 is the membrane surface-charge density $\rho_c(\mathbf{r}_S)$ of Eq. 9 with the partial surface-charge den-

sity $\rho_i(\mathbf{r}_S)$ given in Eq. 7. The grand potential, Eq. 32, now becomes

$$\beta\Omega = -\frac{1}{8\pi\lambda_B}\int_{G_>} d\mathbf{r}(\nabla\phi(\mathbf{r}))^2 - \frac{\tau}{2\pi r_0}\int_{\partial G_z} d\mathbf{r}\phi(\mathbf{r}) - 2c_s\int_{G_>} d\mathbf{r}\cosh\phi(\mathbf{r}) - \frac{1}{a^2}\int_S d\mathbf{r}\ln\left(\sum_{i=1}^{M} c_i a^2(\alpha_i e^{-q_i\Delta\phi(\mathbf{r})} + (1-\alpha_i))\right), \quad (58)$$

which can be transformed into

$$\beta\Omega = \frac{1}{8\pi\lambda_B}\int_{G_>} d\mathbf{r}(\nabla\phi(\mathbf{r}))^2 + 2c_s\int_{G_>} d\mathbf{r}[\phi(\mathbf{r})\sinh\phi(\mathbf{r}) - \cosh\phi(\mathbf{r})] - \frac{1}{a^2}\int_S d\mathbf{r}\ln\left(\sum_{i=1}^{M} c_i a^2(\alpha_i e^{-q_i\Delta\phi(r)} + (1-\alpha_i))\right). \quad (59)$$

We solve the BVP in Eq. 56 numerically with a commercial finite-element program. To improve the resolution, we have first transformed the region $G_>$ onto a rectangular domain by using bicylindrical coordinates. Calculating $\phi(\mathbf{r})$ for a sequence of rod-membrane distances h, inserting it each time into Eq. 59, one obtains $\beta\Omega$ as a function of h, which is nothing but the effective rod-membrane interaction potential. To calculate the distribution of surface ions in the plane of the membrane, the solution ϕ must be placed into Eq. 7 or Eq. 9.

The input parameters of our calculation are τ, r_0 for the cylinder, and λ_B and c_s (or κ) for the electrolyte solution. Fixed throughout are $\lambda_B = 0.714$ nm, and τ and r_0, which are both chosen to simulate a DNA molecule, $\lambda_B\tau = 4$ and $r_0 = 1$ nm. The salt concentration is varied. We first assume that the surface is composed of only two types of lipids, $M = 2$, with valencies q_1 and q_2 and charge ratios α_1 and α_2, but with the same head group size a^2. The mixture is characterized by specifying the surface fraction of species one, c_1a^2, which we choose to be either 0.1 (as in Rädler et al., 1997; Wagner et al., 2000; Kennedy et al., 2000), 0.5 or 1.0. The homogeneous surface-charge density far away from the rod, then, is $\rho_c^\infty a^2 = q_1c_1a^2\alpha_1 + q_2(1 - c_1a^2)\alpha_2$. The head group size of lipids is ranging between 0.4 and 0.8 nm^2 (Shinitzky, 1993; Silver, 1985). In addition to these values, we consider the extreme size of 2 nm^2 for a headgroup to obtain more pronounced finite size effects.

In-plane distribution of mobile surface groups for an almost adsorbed DNA molecule

We first concentrate on the mobility of the surface groups; effects arising from the additional dissociation are discussed later. Let us start by considering a rod that almost touches the x–y plane, i.e., $h = r_0 + 0.1$ nm. The plane is composed of a mixture of positively charged ($\alpha_1 = 1$, $q_1 = 1$) and neutral ($\alpha_2 = 0$, $q_2 = 0$) mobile surface groups, and we calculate from Eqs. 56 and 39 the distribution of the charged surface groups in the plane of the membrane.

This distribution is translationally invariant along the axis of the cylinder and has a mirror symmetry with respect to the y–z plane, so that it suffices to plot the distribution in the direction of the positive x axis. Figure 1 shows the in-plane distribution of the charged surface groups $\rho_1(x)/c_1$ for different salt concentrations ($\kappa^{-1} = 0.3$, 1, 10, and 100 nm) and different head-group sizes ($a^2 = 0.4$ nm^2 and $a^2 = 2$ nm^2). The surface fractions are $c_1a^2 = 0.1$ (Fig. 1 *A* and *B*) and $c_1a^2 = 0.5$ (Fig. 1, *C* and *D*). $\kappa^{-1} = 1$ nm corresponds to the physiological salt concentration of 0.1 M, whereas $\kappa^{-1} = 100$ nm is about the degree of de-ionization that can be achieved with modern ion-exchangers.

Due to their mobility, the positively charged surface groups can move to the negatively charged cylinder adsorbed at $x = 0$. As in a perfect bulk environment, the cylinder is screened by oppositely charged ions, but now this is a screening of ions that are confined to the plane. Clearly, such a 2D screening cannot be perfect, and the total numbers of screening surface groups is smaller than the total number of charges on the cylinder. In other words, there are still mobile ions of the electrolyte solution involved in the screening of the cylinder. The distributions in Fig. 1 reveal that the ratio of screening electrolyte ions to screening surface ions is not a fixed quantity, but changes with a^2 and κ^{-1}. For example, if the concentration of salt in bulk is reduced, the number of screening surface ions increases.

Mobility allows an inhomogeneous surface ion distribution, and, locally, the surface density of ions can become much larger than it is at infinite x. Mobility actually means that neutral surface groups are replaced by charged groups, or vice versa. This process naturally ends if all possible replacements are made. In the case of $c_1a^2 = 0.1$, this happens at a density of $\rho_1/c_1 = 10 = 1/(c_1a^2)$ when all neutral groups are replaced by charged groups. This limit, as we can see from Fig. 1 *B*, is reached for $a^2 = 2$ nm^2, $\kappa^{-1} = 100$ nm, i.e., only for very large surface groups or low salt concentration. If this packing effect sets in, it has a pronounced impact on the whole distribution, which we see is spread over a much larger x range now. This can be attributed to the fact that, due to the packing effect, the surface

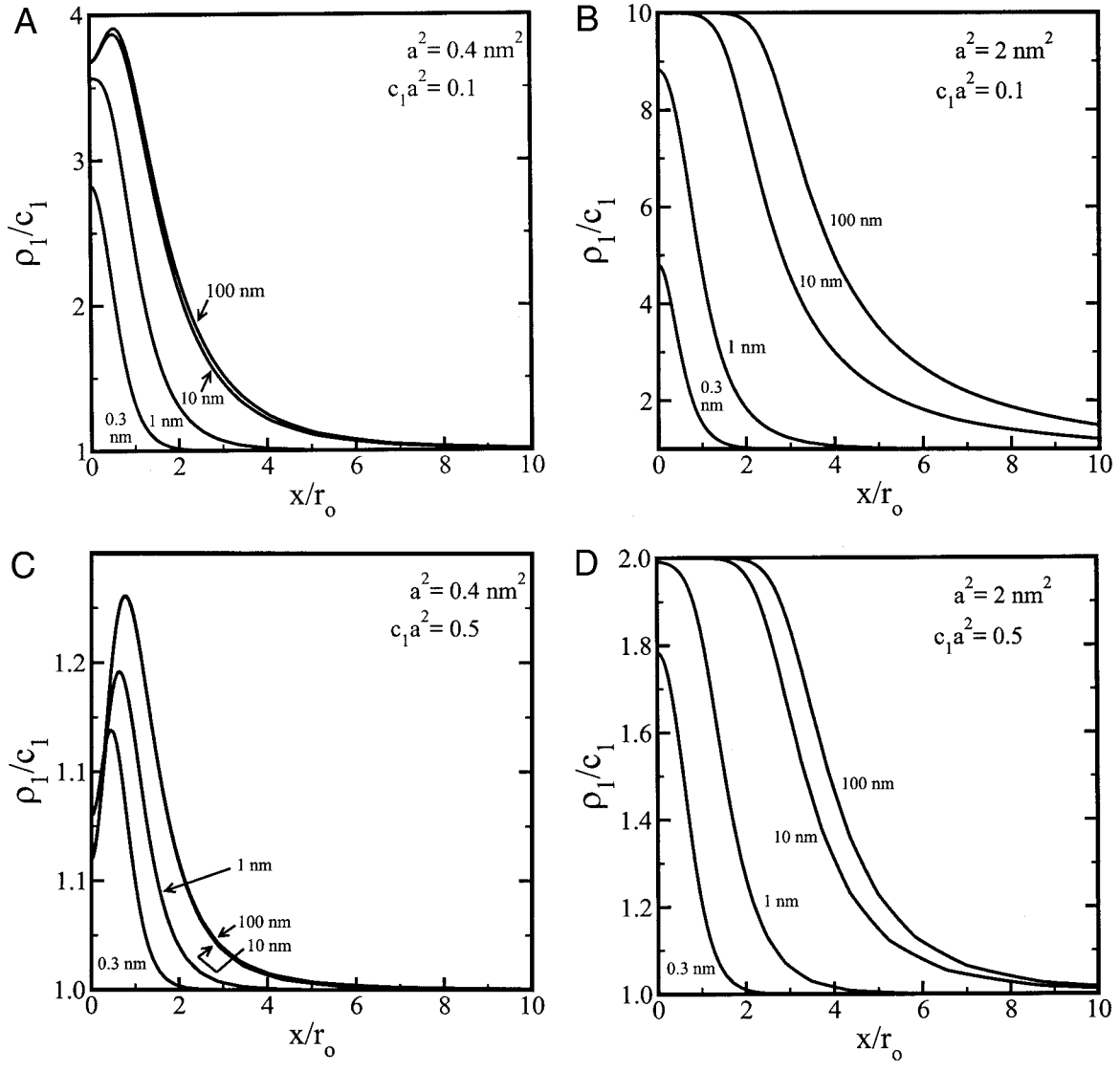

FIGURE 1 Surface-charge density distribution $\rho_1(x)/c_1$ of mobile, positively charged surface groups in a membrane, for a negatively charged rod (DNA molecule), which almost touches the membrane ($h = r_0 + 0.1$ nm) at $x = 0$. The surface fractions of positively charged surface groups are $c_1a^2 = 0.1$ in (*A*) and (*B*) and $c_1a^2 = 0.5$ in (*C*) and (*D*). For each surface fraction, we consider surface groups of size $a^2 = 0.4$ nm^2 and $a^2 = 2$ nm^2. The numbers at the curves specify the salt concentration κ^{-1}. For low salt concentration ($\kappa^{-1} = 10$ and 100 nm), one can clearly recognize the effect due to the packing of the surface groups (Panels *B* and *D*). The packing effect results in a spread of the distribution over a much larger x range.

ions can no longer screen the fixed cylinder charges in the best way possible so that the Coulomb field becomes longer ranged now.

Another interesting feature of the curves in Fig. 1 is the peak in the density distribution at $x = 1$ nm for $\kappa^{-1} = 100$ nm and $a^2 = 0.4$ nm^2. Because the electrolyte ions are hardly taking part in the screening of the cylinder and the surface ions are too small for any packing effect to occur, the distribution can accurately trace the 2D projection of the electric field of the cylinder; the peak occurs at $x = r_0$. The distribution for $x < 1$ nm follows just the curvature of the cylinder. Increasing the salt concentration in the electrolyte destroys this effect, because the 3D screening of the electrolyte ions between the rod and the membrane now prevents that the shape of the rod can be seen by the surface ions.

What determines the density value at $x = 0$? To understand this value, we consider the dimensionless quantity $\lambda_B\zeta(x) := 2\pi r_0\lambda_B\rho_1(x)$ by means of which ρ_1 becomes directly comparable to the line charge density $\lambda_B\tau$ on the cylinder. Figure 2 shows $\lambda_B\zeta(x)$ for $a^2 = 0.4, 0.8, 2$ nm^2 at an intermediate salt concentration of $\kappa^{-1} = 50$ nm ($c_1a^2 = 0.1$). The plot reveals that the surface-charge density distribution ρ_1 at $x = 0$ reaches a value such that $\lambda_B\zeta(0)$ becomes equal to the line-charge density $\lambda_B\tau = 4$ of the cylinder, which clearly means optimal screening of the cylinder

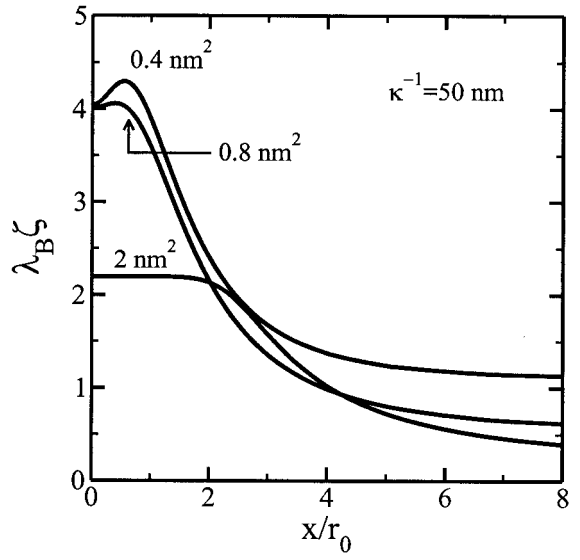

FIGURE 2 In-plane density distribution as in Fig. 1, but now plotted using the dimensionless quantity $\lambda_B\zeta(x) = 2\pi r_0\lambda_B\rho_1(x)$. The salt concentration is $\kappa^{-1} = 50$ nm. If the size of the surface group is small enough, the surface charge density in the vicinity of the cylinder matches the charge density on the cylinder.

charges. A prerequisite for this optimal screening however is that the surface ions are small enough to be packed so closely. For example, the $a^2 = 2$ nm^2 curve, with $\lambda\zeta(0)$ remaining well below 4, demonstrates that packing effects can prevent optimal screening.

With this result, we can derive a criterion beyond which value of a^2, the finite size of the surface groups becomes effective. Using $\lambda_B\zeta(0) = \lambda_B\tau$ and $\lambda_B\zeta(0) = 2\pi r_0\lambda_B\rho_1(0)$, plus the fact that the maximum density of ions in the surface is a^{-2}, we find that a^2 must be greater than $2\pi r_0\tau^{-1}$ for packing effects to occur, something that we have successfully checked by explicit calculations for other values of r_0 and τ. The critical value for a^2 is 1.12 nm^2 for a DNA molecule with $\lambda_B\tau = 4$ and a radius of $r_0 = 1$ nm, and is thus much larger then the head groups of typical lipids. A saturation effect like that shown by the curve for $a^2 = 2$ nm^2 in Fig. 2 is therefore not to be expected in real DNA/membrane systems. Other finite size effects, however, are possible; for instance, the disappearance of the peak at $x = r_0$ in going from $a^2 = 0.4$ nm^2 to $a^2 = 0.8$ nm^2 in Fig. 2.

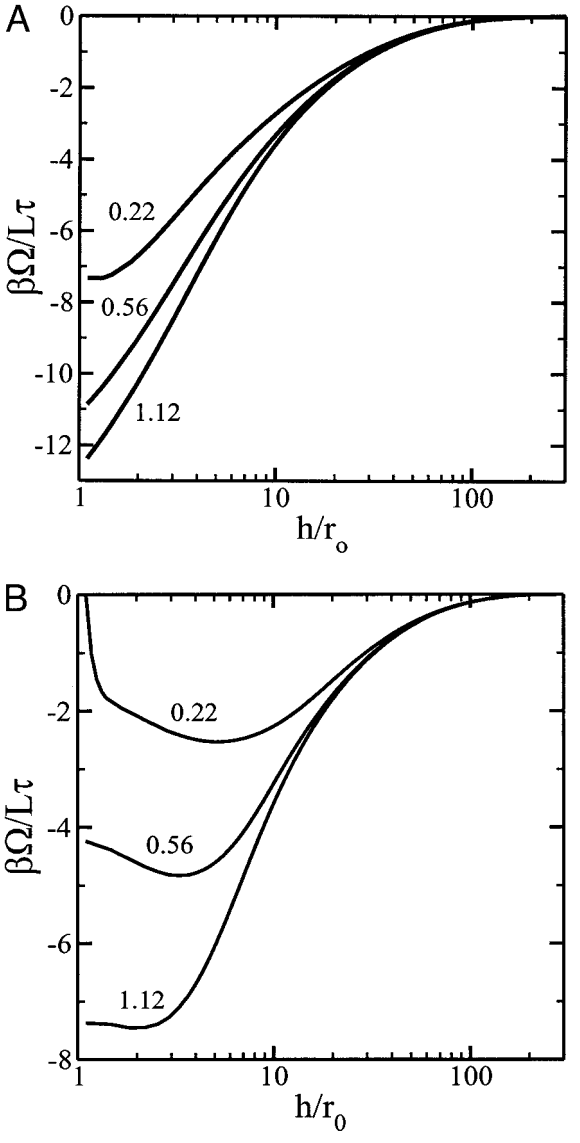

FIGURE 3 Effective DNA–membrane interaction potentials per unit charge on the cylinder for (*A*) mobile and (*B*) immobile surface ions (*L* denotes the length of the cylinder). Three different homogeneous charge densities $\beta\zeta^\infty = 2\pi r_0\lambda_B c_1$ are considered (specified by the numbers at the curves), which, in the case of mobile ions, correspond to a head group size of $a^2 = 0.4$, 0.8, and 2 nm^2 and a surface fraction of $c_1a^2 = 0.1$. The salt concentration is again $\kappa^{-1} = 50$ nm. The mobility of the surface groups leads to an increased rod–membrane Coulomb attraction (*A*) in comparison to the immobile case (*B*).

Effective interaction for variable rod-membrane distances

We now vary the rod-wall distance h. In the following, we present all quantities per unit charge on the cylinder. In Fig. 3, we show the grand potential as a function of h, for $\kappa^{-1} = 50$ nm, $c_1a^2 = 0.1$, $a^2 = 0.4$, 0.8, and 2 nm^2. This is the set of parameters already used before and the in-plane ion distribution corresponding to the point $h = r_0$ in Fig. 3 *A* is given in Fig. 2. The interaction energy at infinite distance from the membrane, $\beta\Omega(h = \infty)$, is subtracted. The surface charge density at infinity is conveniently characterized by $\lambda_B\zeta^\infty = 2\pi r_0\lambda_B c_1$ which is 0.22, 0.56, and 1.12 for $a^2 = 2$, 0.8, and 0.4 nm^2. In Fig. 3 *B*, we calculate the effective interaction for the same surface-charge densities $\lambda_B\zeta^\infty = 0.22$, 0.56, and 1.12, but now for immobile ions. For that, we have to solve Eq. 56 with $\rho_c = c_1$.

Let us first discuss Fig. 3 *B*. If there were no interfacial charges and no screening ions at all, the boundary condition at *S* in Eq. 56 would reduce to $\mathbf{n}_{=}\nabla\phi(\mathbf{r}) = 0$, which can be satisfied with the auxiliary construction of image charges, i.e., by the assumption that, at $z < 0$, there is a perfect mirror image of all charges at $z > 0$. Then the x–y plane is a symmetry plane and $\mathbf{n}_{=}\nabla\phi(\mathbf{r})$ must vanish. Clearly, a rod approaching the plane will, at some stage, become aware of its own image, which must result in an repulsive interaction. The interplay of this image–charge repulsion and the direct (screened) Coulomb attraction between the membrane and the rod charges leads to the minimum in the effective interaction potentials of Fig. 3 *B*. Increasing $\lambda_B\zeta^{\infty}$, while leaving $\lambda_B\tau$ constant, enhances the direct Coulomb attraction, but leaves the indirect repulsive image–charge interaction unchanged. As is evident from the three curves of Fig. 3 *B*, the minimum then becomes deeper and its position moves toward the plane. For even larger surface-charge densities ($\lambda_B\zeta^{\infty} > 1.9$), the minimum will be directly at the membrane.

Comparison of Fig. 3, *A* and *B*, now shows that surface-group mobility considerably increases the effective DNA–membrane attraction. The positions of the energy minima of all three curves in Fig. 3 *B* are shifted toward the contact value in Fig. 3 *A*, and their depth is a factor 1.5–3 times larger than before. The reason for this follows from an observation made in Fig. 1: locally, the surface density of mobile surface ions can become much larger than it is at infinite x (and thus for immobile surface groups) and this leads, globally, to an increased rod–membrane Coulomb attraction.

Figure 4 shows the result of our numerical PB solution for the effective rod–membrane interaction in the case of a membrane with immobile charged lipids and a surface charge density $c_1 = 0.1\ \mathrm{nm}^{-2}$ (*broken line*). The screening length in this case is fixed at $\kappa^{-1} = 10$ nm. Here, we compare this curve with various approximations that can be made. On the linear level, the electrostatic interaction energy between a negatively charged line and charged wall that is impenetrable to salt ions is given per unit charge on the line by

$$\frac{\beta\Omega_{\mathrm{DH}}}{L\tau} = -\frac{4\pi\lambda_B c_1}{\kappa}\exp(-h\kappa), \qquad (60)$$

where h denotes the distance of the charged line from the charged wall and L the length of the line. This function is denoted by *DH* in the Fig. 4. The self-energy of a charged line close to a wall that is impenetrable to salt ions has been calculated in Netz (1999) and is given by

$$\frac{\beta\Omega_s}{L\tau} = \lambda_B\tau K_0(2\kappa h), \qquad (61)$$

and denoted by K_0 in Fig. 4. On the linear level, it is permitted to add Eqs. 60 and 61, and the result is denoted by

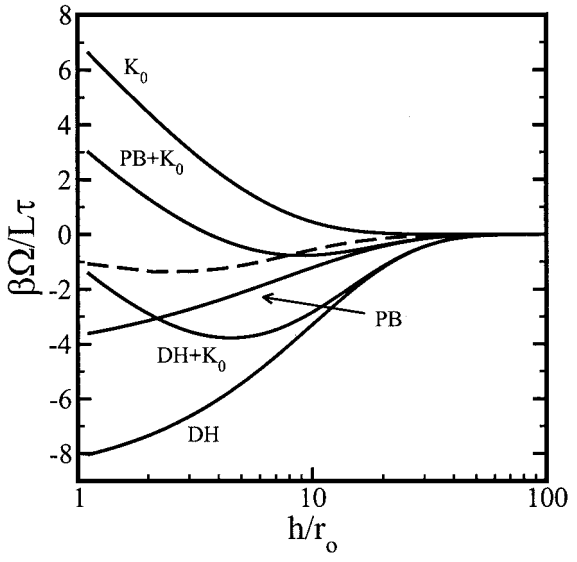

FIGURE 4 Comparison of the numerical solution of the PB equation in Eq. 56 (*broken line*) with various others approximations (which neglect the finite diameter of the cylinder) for a surface charge density $c_1 = 0.1\ \mathrm{nm}^{-2}$ and a screening length $\kappa^{-1} = 1$ nm. Results based on the Debye–Hückel approximation (*DH*) and the Poisson–Boltzmann (*PB*) theory for a line charge are shown. We also show the self-energy of a line charge near a wall that is impenetrable to ions (K_0) and the sum of Debye–Hückel and Poisson–Boltzmann approximation with the self energy, ($DH + K_0$) and ($PB + K_0$), respectively.

$DH + K_0$ in Fig. 4. All these approximations neglect nonlinear effects, but also the fact that the cylinder is impenetrable to ions. Nonlinear effects can be taken into account by using the PB potential of a charged wall. The interaction of a line charge with the unperturbed double layer of a charged wall reads

$$\frac{\beta\Omega_{\mathrm{PB}}}{L\tau} = -2\ln\left[\frac{1+\tanh(\phi_0/4)e^{-\kappa h}}{1-\tanh(\phi_0/4)e^{-\kappa h}}\right], \qquad (62)$$

which is labeled by surface *PB* in Fig. 4. Here, ϕ_0 denotes the surface potential on the membrane. We also show the sum of the PB potential and the DH self-energy of a line, denoted by $PB + K_0$. The PB curve describes the true nonlinear free energy, which includes ion-exclusion effects (*broken line*) best, as one would expect. Despite the fact that the charge density on the wall is very small, the linear approximation for the electrostatic interaction energy Ω_{DH} differs clearly from the nonlinear expression Ω_{PB}, as can be seen by comparison of the curves *DH* and *PB* in Fig. 4. The linear solution overestimates the interaction between rod and wall. This demonstrates that nonlinear effects are important and a linearization is not allowed for the parameters used here. The linear approximation becomes better if one increases the salt concentration κ^{-1}.

Because rod and plane, and thus their associated double layers are oppositely charged, the two double layers will start to dissolve each other when the rod–plane distance

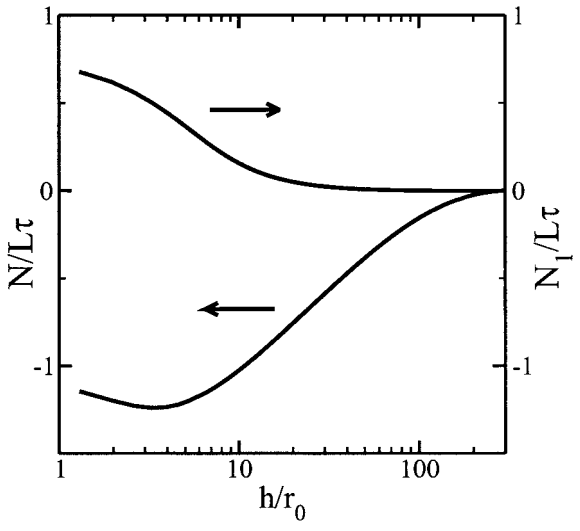

FIGURE 5 Change of total number of screening salt ions per unit charge on the cylinder (*lower curve*, *left scale*) and of screening surface ions (*upper curve*, *right scale*) as a function of the DNA–membrane distance h ($c_1a^2 = 0.1$, $a^2 = 0.8$ nm^2, $\kappa^{-1} = 50$ nm).

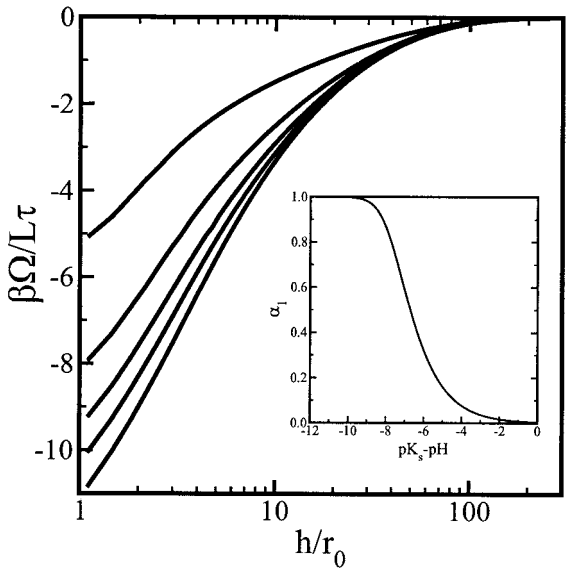

FIGURE 6 Effect of varying the degree of dissociation α on the effective DNA–membrane interaction per unit charge on the cylinder. α_1 is 0.1, 0.3, 0.5, 0.7, and 1 from top to bottom. The inset shows α_1 as a function of the difference $pK_s - pH$ ($c_1a^2 = 0.1$, $a^2 = 0.8$ nm^2, $\kappa^{-1} = 50$ nm).

becomes small enough for the two double layers to overlap. Because the fixed charges of rod and plane then begin to screen each other, mobile electrolyte ions of these double layers are no longer needed to screen the fixed charges and can disappear into the reservoir. This release of ions can be seen in Fig. 5, where we plotted the change in the total number of screening electrolyte ions per unit charge on the cylinder, given by

$$\frac{N}{L\tau} = \frac{1}{L\tau}\int_{G_>} d\mathbf{r}[\rho_+^e(\mathbf{r}) + \rho_-^e(\mathbf{r}) - 2c_s], \qquad (63)$$

as a function of the distance h. This is a negative number for all distances, but with a minimum at some finite value of h due to the image-charge effect. Connected with this release of counterions, there is an enthalpy gain of the whole system, which leads to an additional attractive rod–membrane force, the counterion release force (Fleck and von Grünberg, 2001). In addition, we show, in Fig. 5, the change,

$$\frac{N_1}{L\tau} = \frac{1}{L\tau}\int_S d\mathbf{r}[\rho_1(\mathbf{r}) - c_1], \qquad (64)$$

in the total number of surface ions (integral over ion distributions like in Fig. 1) as a function of h. These are positive numbers; surface ions flow in from the reservoir to help screen the cylinder. The cylinder becomes visible for the surface ions only after the 3D screening of the rod is sufficiently reduced; that explains why the disappearance of electrolyte ions sets in earlier than the appearance of additional surface ions. Closer inspection shows that the two curves $N_1(h)$ and $N(h)$ are, in fact, intimately related to each other, any change in one quantity affects the other. In essence, Fig. 5 describes the transition from the 3D bulk ion screening to the 2D surface ion screening.

Up to now we have completely ignored the dissociation as a competing charge-regulating mechanism. Let us now consider the effect of the variables α_i, a quantity that, in an experiment, can be regulated by changing the pH value of the solution (see Eqs. 2 and 3). Figure 6 displays the effective interaction when α_1 is varied from 0.1 to 1.0. In this calculation, Eq. 39 is used for ρ_c in Eq. 56, and a^2 is fixed to 0.8 nm^2 in a mixture of neutral ($\alpha_2 = 0$) and positively charged surface groups ($c_1a^2 = 0.1$, $\kappa^{-1} = 50$ nm). The curve for $\alpha_1 = 1.0$ is the same as the curve for $a^2 = 0.8$ nm^2 ($\lambda_B\zeta^\infty = 0.56$) in Fig. 3 *A*. The inset of Fig. 6 shows α_1 as a function of the difference $pK_s - pH$ to render this graph useful to experimentalists. (Looking at Eq. 3, it becomes obvious that, to calculate α_1 as a function of $pK_s - pH$, it is necessary to determine ϕ^∞. This can be done by solving the Graham equation: $2\kappa \sinh(\phi^\infty/2) = 4\pi\lambda_B/(e^{\ln 10(pK_s - pH)\phi^\infty} + 1)$ for ϕ^∞.) We have already noted in the discussion of Eq. 39 that, in such a two-component mixture with one group type being neutral, variations of α are equivalent to changes in c_1a^2. Thus, Fig. 6 can also be understood as the variation of the effective interaction in response to changes of the surface fraction c_1a^2. The message of the plot is that increasing α (or increasing c_1a^2) makes the interaction more attractive because any increase of the homogeneous surface charge density $\lambda_B\zeta^\infty$ causes an increase of the direct Coulomb interaction between the rod

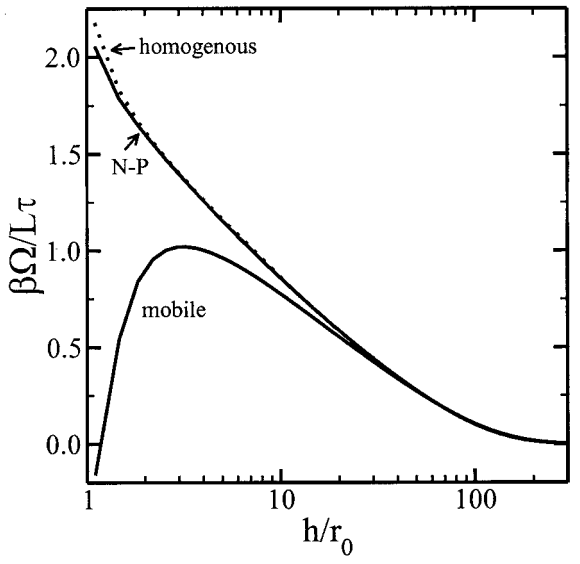

FIGURE 7 DNA–membrane interaction for three different models of a membrane. Case I (*mobile*): the model membrane is composed of three types of mobile surface groups: negatively charged, neutral and dissociable. Case II (*N-P*): membrane charges result from dissociation as in case I, but surface ions are immobile (Ninham–Parsegian boundary condition). Case III (*homogeneous*): charges are fixed, surface ions are immobile. In all three cases, the homogeneous surface-charge density far away from the DVA is equal and corresponds to an effective homogeneous charge density of $\rho_c = -1/4.8$ nm^2 ($\kappa^{-1} = 50$ nm).

and the membrane, something we have already learned from Fig. 3 *A*, where $\lambda_B\zeta^\infty$ was varied by changing a^2.

We still need to show that, allowing for both charge-regulating mechanisms, mobility plus dissociation (case I), makes an effect and leads to an interaction potential that is different from the one based on only one such mechanism, for instance, dissociation (case II). The latter is realized by using Eqs. 4 and 9 in the boundary condition at S in Eq. 56, a trivial generalization of Eq. 41 used first by Ninham and Parsegian (1971). We now take a membrane made of three different components, with surface fractions $c_1a^2 = c_2a^2 = c_3a^2 = 0.33$, valencies $q_3 = -q_2 = 1$, $q_1 = 0$, and $a^2 = 0.8$ nm^2 ($\kappa^{-1} = 50$ nm). The components are neutral, fully, and only partially charged ($\alpha_1 = 0$, $\alpha_2 = 1.0$, $\alpha_3 = 0.5$). Thus the membrane is (on average) negatively charged. The same values for α_i are taken in Eq. 4 where the c_i are chosen such that the homogeneous surface-charge density $\lambda_B\zeta^\infty$ is identical in case I and II. As a third case, we calculate the effective interaction between the DNA and a homogeneously charged membrane composed of immobile surface groups, that is, we used $\rho_c = -\zeta^\infty/(2\pi r_0)$ in Eq. 56, with ζ^∞ being the same as in case I and II.

As we noticed already, in Fig. 7, surface-group mobility takes effect at short distances, that is, long after the rod has started to interact with the membrane. For larger distances, the specific properties of the membrane are obviously unimportant; only the characteristic of the double-layer in front of the membrane is essential. But, because the double-layers are determined by nothing but the homogeneous surface-charge densities that are the same in all three cases, the interaction potentials in Fig. 7 must coincide for larger distances. However, for smaller distances a drastic change sets in: positively charged, mobile ions ($q_3 = +1$) flow into that region of the interface where $\Delta\phi(\mathbf{r}_S) \neq 0$ and replace the neutral groups, while ions of the second type ($q_2 = -1$) escape from this region. The surface, though, on average, still negatively charged, becomes locally positively charged so that the DNA–membrane interaction becomes attractive. This change from repulsion to attraction is a remarkable result and underlines the importance of surface-group mobility: ignoring the ion's ability to move within the plane of the membrane as done in case II and III, one comes to the wrong conclusion that the interaction is repulsive. In case II, the Ninham–Parsegian case, the in-plane ion distribution adapts to the electric field of the DNA rod, with a strongly enhanced dissociation in regions where $\Delta\phi(\mathbf{r}_S) \neq 0$. The membrane becomes locally neutral, and the resulting effective interaction is repulsive at all distances. The spatially dependent dissociation rate does not lead to a change of sign of the effective force, but just, for very short distances, to a small reduction of the interaction potential in comparison to the homogeneously charged membrane.

CONCLUSION

Charges on membranes arise from a pH-dependent chemical reaction on the headgroups of phospholipids. If another charged object approaches the membrane, a local adaption of the degree of dissociation of the surface groups is an effective way for the system to lower its total energy. Theoretically, this case is treated by solving the PB equation with the traditional charge-regulation boundary condition first introduced by Ninham and Parsegian (1971). However, a realistic model of a membrane must also take account of the fluidity of membranes. The in-plane mobility of membrane components represent a second and additional charge-regulating mechanism. The appropriate boundary condition dealing with this case is derived and discussed in this work.

Using this boundary condition, we have numerically calculated the interaction of a stiff DNA molecule with a model membrane consisting of mobile surface groups whose state of charge depends on the pH of the solution. Figure 7 represents perhaps the best summary of our results: it shows that modeling the membrane by a homogeneously charged surface is adequate only if one is interested in the interaction at larger distances where the particulars of the membrane can be ignored. However, at short distances, membrane fluidity can have a considerable impact on the DNA adsorption behavior. Figure 7 shows that, in this distance regime, the interaction of the DNA with a membrane composed of mobile surface groups differs appreciably from the interaction of a DNA with membranes having

immobile surface charges. We thus see that surface-group mobility can lead to such counterintuitive phenomena as the adsorption of a negatively charged DNA onto a like-charged membrane.

Neither the idea of taking account of the lipid's ability to move, nor the idea of including the charge-regulating chemical reactions at the membrane's surface, are new, but have appeared in literature before as we have repeatedly stressed in the text. New is, and that is the contribution of this work, the combination of both aspects: surface group mobility and dissociation as two competing mechanisms to regulate the surface charge density of the membrane.

In this paper, we assumed implicitly as in the DLVO-Theory that van der Waals forces and electrical double-layer forces are additive and can be treated independently. This is generally not true as pointed out by (Ninham and Yaminsky, 1997; Ninham, 1999). A more detailed description should take into account the intimate relation between electrostatic and van der Waals forces. For a discussion of van der Waals forces in bilayer systems, see Kékicheff and Ninham (1990), Nylander et al. (1994), and Attard et al. (1988b). A complete theory should also include the effect of ion specificity, dissolved gas, and the role of the buffer as discussed in Kim et al. (2001). Nevertheless, we believe that, within the known limitations of DLVO theory, our results, in particular the derived boundary condition, should be useful in more elaborate PB calculations of proteins, DNA, and cell membranes.

Acknowledgments

Financial support from the Deutsche Forschungsgemeinschaft (SFB 513) is gratefully acknowledged. C.F. thanks Reinhard Sipowsky for his kind hospitality at the Max-Planck-Institut für Kolloid-und Grenzflächenforschung.

REFERENCES

Almeida, P., and W. Vaz. 1995. Lateral diffusion in membranes. *In* Structure and Dynamics of Membranes. R. Lipowsky and E. Sackmann, editors. North Holland, Amsterdam. 305–357.

Andelman, D. 1995. Electrostatic properties of membranes: the Poisson–Boltzmann theory. *In* Structure and Dynamics of Membranes. R. Lipowsky and E. Sackmann, editors. North Holland, Amsterdam. 603–642.

Attard, P., R. Kjellander, D. Mitchell, and B. Jönsson. 1988a. Electrostatic fluctuation interaction between neutral surfaces with adsorbed, mobile ions or dipoles. *J. Chem. Phys.* 89:1664–1670.

Attard, P., D. J. Mitchell, and B. W. Ninham. 1988b. The attractive forces between polar lipid bilayers. *Biophys. J.* 53:457–460.

Barrat, J., and J. Joanny. 1996. Theory of polyelectrolyte solutions. *Adv. Chem. Phys.* 94:1–66.

Behr, J. P. 1994. Gene transfer with synthetic cationic amphiphiles—prospects for gene-therapy. *Bioconjugate Chem.* 5:382–389.

Borukhov, I., D. Andelman, and H. Orland. 1997. Steric effects in electrolytes: a modified Poisson–Boltzmann equation. *Phys. Rev. Lett.* 79:435–438.

Borukhov, I., D. Andelman, and H. Orland. 2000. Adsorption of large ions from an electrolyte solution: a modified Poisson–Boltzmann equation. *Electrochimica Acta.* 46:221–233.

Bruinsma, R., and J. Mashl. 1998. Long-range electrostatic interaction in DNA-cationic complexes. *Europhys. Lett.* 41:165–170.

Chan, D., T. Healy, and L. White. 1976. Electrical double layer interactions under regulation by surface ionization equilibria—dissimilar amphoteric surfaces. *J. Chem. Soc. Faraday Trans.* 72:2844–2866.

Cooper, G. 2000. The Cell, a Molecular Approach, ASM Press, Washington, DC.

Dan, N. 1997. Multilamellar structures of DNA complexes with cationic liposomes. *Biophys. J.* 73:1842–1846.

Fang, Y., and J. Yang. 1997. Effect of cationic strength and species on 2-D condensation of DNA. *J. Phys. Chem. B.* 101:3453–3456.

Felgner, P. L., T. Gadek, M. Holm, R. Roman, H. W. Chan, M. Wenz, J. Northrop, G. Ringold, and M. Danielsen. 1987. Lipofection—a highly efficient lipid-mediated DNA-transfection procedure. *Proc. Natl. Acad. Sci. U.S.A.* 84:7413–7417.

Felgner, J., R. Kumar, C. Sridhar, C. J. Wheeler, Y. Tsai, R. Border, P. Ramsey, M. Martin, and P. Felgner. 1994. Enhanced gene delivery and mechanism studies with a novel series of cationic lipid formations. *J. Biol. Chem.* 269:2550–2563.

Firshein, W. 1989. Role of the DNA membrane complex in prokaryotic DNA-replication. *Annu. Rev. Microbiol.* 43:89–120.

Fleck, C., and H. von Grünberg. 2001. Counterion evaporation. *Phys. Rev. E.* 63:061804.

Fleer, G., M. C. Stuart, J. Scheutjens, T. Cosgrove, and B. Vincent. 1993. Polymers at Interfaces. Chapman and Hall, London.

Fogden, A., and B. W. Ninham. 1991. The bending modulus of ionic lamellar phases. *Langmuir.* 7:590–601.

Gelbart, W., R. Bruinsma, P. Pincus, and V. Parsegian. 2000. DNA-inspired electrostatics. *Physics Today.* 53:38–42.

Guttman, G., and D. Andelman. 1993. Electrostatic interactions in two-component membranes. *J. Phys. II (France).* 3:1411–1425.

Harries, D., S. May, W. M. Gelbart, and A. Ben-Shaul. 2000. Structure, stability, and thermo-dynamics of lamelar DNA-lipid complexes. *Biophys. J.* 78:1681–1697.

Healy, T., and L. White. 1978. Ionizable surface group models of aqueous interfaces. *Adv. Colloid. Interf. Sci.* 9:303–315.

Healy, T. W., D. Chan, and L. R. White. 1980. Colloidal behaviour of materials with ionizable group surfaces. *Pure Appl. Chem.* 52: 1207–1222.

Kékicheff, P., and B. W. Ninham. 1990. The double-layer interaction in asymmetric electrolytes. *Europhys. Lett.* 12:471–474.

Kennedy, M., E. Pozharski, V. Rakhmanova, and R. MacDonald. 2000. Factors governing the assembly of cationic phospholipid DNA complexes. *Biophys. J.* 78:1620–1633.

Kim, H.-K., E. Tuite, B. Norden, and B. W. Ninham. 2001. Co-ion dependence of DNA nuclease activity suggests hydrophobic cavitation as a potential source of activation energy. *Eur. Phys. J. E.* 4:411–417.

Koltover, I., T. Salditt, J. O. Rädler, and C. R. Safinya. 1998. An inverted hexagonal phase of cationic liposome-DNA complexes related to DNA release and delivery. *Science.* 281:78–80.

Koltover, I., T. Salditt, and C. Safinya. 1999. Phase diagram, stability and overcharging of lamellar cationic lipid DNA self assembled complexes. *Biophys. J.* 77:915–924.

Kralj-Iglic, V., and A. Iglic. 1996. A simple statistical mechanical approach to the free energy of the electrical double layer including the excluded volume effect. *J. Phys. II (France).* 6:477–491.

Lasic, D., H. Strey, M. Stuart, R. Podgornik, and P. M. Frederil. 1997. The structure of DNA liposome complexes. *J. Am. Chem. Soc.* 119:832–841.

Lau, A., and P. Pincus. 1998. Charge-fluctuation-induced nonanalytic bending rigidity. *Phys. Rev. Lett.* 81:1338–1341.

Löwen, H., and J. Hansen. 2000. Effective interactions between electric double layers. *Annu. Rev. Phys. Chem.* 51:209–242.

Maier, B., and J. O. Rädler. 1999. Conformation and self-diffusion of single DNA molecules confined to two dimensions. *Phys. Rev. Lett.* 82:1911–1914.

Mashl, R., N. Gronbech-Jensen, M. Fitzsimmons, M. Lütt, and D. Li. 1999. Theoretical and experimental adsorption studies of polyelectrolytes on an oppositely charged surface. *J. Chem. Phys.* 110:2219–2225.

Mashl, R. J., and N. Gronbech-Jensen. 1998. Effective interactions between rigid polyelectrolyte and like-charged planar surface. *J. Chem. Phys.* 109:4617–4623.

May, S., D. Harries, and A. Ben-Shaul. 2000a. Lipid demixing and protein–protein interactions in the adsorption of charged proteins on mixed membranes. *Biophys. J.* 79:1747–1760.

May, S., D. Harries, and A. Ben-Shaul. 2000b. The phase behavior of cationic lipid-DNA complexes. *Biophys. J.* 78:1681–1697.

Menes, R., P. Pincus, R. Pittman, and N. Dan. 1998. Fields generated by a rod adsorbed on an oppositely charged surface. *Europhys. Lett.* 44: 393–398.

Netz, R. 1999. Debye–Hückel theory for interfacial geometries. *Phys. Rev. E.* 60:3174–3182.

Netz, R. 2000. Debye–Hückel theory for slab geometries. *Eur. Phys. J. E.* 3:131–141.

Netz, R., and H. Orland. 1999. Field theory for charged fluids and colloids. *Europhys. Lett.* 45:726–732.

Netz, R., and H. Orland. 2000. Beyond Poisson–Boltzmann: fluctuation effects and correlation functions. *Eur. Phys. J. E.* 1:203–214.

Nguyen, T. T., A. Y. Grosberg, and B. I. Shklovskii. 2001. Screening of a charged particle by multivalent counterions in salty water: strong charge inversions. J Chem. Phys. 113:1110–1125.

Ninham, B., and V. Parsegian. 1971. Electrostatic potential between surfaces bearing ionizable groups in ionic equilibrium with physiologic saline solution. *J. Theor. Biol.* 31:405–421.

Ninham, B. W. 1999. On progress in forces since the DLVO theory. *Adv. Colloid Interface Sci.* 83:1–17.

Ninham, B. W., and V. Yaminsky. 1997. Ion binding and ion specificity: the Hoffmeister effect and Onsager and Lifshitz theories. *Langmuir.* 13:2097–2108.

Nylander, T., P. Kékicheff, and B. W. Ninham. 1994. The effect of solution behavior of insulin on interactions between adsorbed layers of insulin. *J. Colloid Interface Sci.* 164:136–145.

Parsegian, V. A., and D. Gingell. 1972. On the electrostatic interaction across a salt solution between two bodies bearing unequal charges. *Biophys. J.* 12:1193–1204.

Pincus, P., and S. Safran. 1998. Charge fluctuation and membrane attractions. *Europhys. Lett.* 42:103–108.

Rädler, J. O., I. Koltover, T. Salditt, and C. R. Safinya. 1997. Structure of DNA-cationic liposome complexes: DNA intercalation in multilamellar membranes in distinct interhelical packing regimes. *Science.* 275: 810–815.

Sackman, E., and R. Lipowsky. 1995. Structure and Dynamic of Membranes. North Holland, Amsterdam.

Salditt, T., I. Koltover, J. O. Rädler, and C. Safinya. 1997. Two-dimensional smetic ordering of linear DNA chains in self-assembled DNA-cationic liposome mixtures. *Phys. Rev. Lett.* 79:2582–2585.

Sens, P., and J. F. Joanny. 2000. Counterion release and electrostatic adsorption. *Phys. Rev. Lett.* 84:4862–4865.

Shinitzky, M. 1993. Biomembranes. VCH, Weinheim, Germany.

Silver, B. L. 1985. The Physical Chemistry of Membranes. Allen & Unwin, London.

Templeton, N., D. Lasic, P. Frederik, H. Strey, D. D. Roberts, and G. Pavlakis. 1997. Improved DNA-liposome complexes for increased systemic delivery and gene-expression. *Nature Biotech.* 15:647–652.

Verma, I., and N. Somia. 1997. Gene Therapy—Promises, Problems and Prospects. *Nature.* 389:239–242.

Wagner, K., D. Harries, S. May, V. Kahl, J. Rädler, and A. Ben-Shaul. 2000. Direct evidence for counterion release upon cationic lipid-DNA condensation. *Langmuir.* 26:303–306.